Structural Engineering and Mechanics, *Vol. 63, No. 5 (2017) 683-689*
DOI: https://doi.org/10.12989/sem.2017.63.5.683

A refined hyperbolic shear deformation theory for bending of functionally graded beams based on neutral surface position

Nafissa Zouatnia[1], Lazreg Hadji*[2] and Amar Kassoul[1]

[1]*Department of Civil Engineering, Laboratory of Structures, Geotechnics and Risks (LSGR), Hassiba Benbouali University of Chlef, Algeria, BP 151, Hay Essalam, UHB Chlef, Chlef (02000), Algeria*
[2]*Department of Civil Engineering, Ibn Khaldoun University, BP 78 Zaaroura, 14000 Tiaret, Algeria*

(Received December 19, 2016, Revised July 1, 2017, Accepted July 28, 2017)

Abstract. In this paper, a hyperbolic shear deformation theory is presented for bending analysis of functionally graded beams. This theory used in displacement field in terms of thickness co-ordinate to represent the shear deformation effects and does not require shear correction factor, and gives rise to transverse shear stress variation such that the transverse shear stresses vary parabolically across the thickness satisfying shear stress free surface conditions. The governing equations are derived by employing the virtual work principle and the physical neutral surface concept. A simply supported functionally graded beam subjected to uniformly distributed loads and sinusoidal loads are consider for detail numerical study. The accuracy of the present solutions is verified by comparing the obtained results with available published ones.

Keywords: functionally graded; Navier's solution; physical neutral surface; virtual work; sinusoidal loads

1. Introduction

In recent years, astonishing advances in science and technology have motivated researchers towork on newstructural materials. Functionally graded materials (FGMs) are classified as novel composite materials which are widely used in aerospace, nuclear, civil, automotive, optical, biomechanical, electronic, chemical, mechanical, and shipbuilding industries. By gradually varying the volume fraction of constituent materials, their material properties exhibit a smooth and continuous change from one surface to another, thus eliminating interface problems and mitigating thermal stress concentrations. FGMs now have been regarded as one of the most promising candidates for future intelligent composites in various engineering sectors such as aerospace, fast computers, biomedical industry, environmental sensors, etc. FGMs may possess a number of advantages such as high resistance to temperature gradients, significant reduction in residual and thermal stresses, and high wear resistance.

Due to the increased relevance of the FGMs structural components in the design of engineering structures, many studies have been reported on the static, and vibration analyses of functionally graded (FG) beams. Li (2008) investigated static bending and transverse vibration of FGM Timoshenko beams, in which by introducing a new function, the governing equations for bending and vibration of FGM beams were decoupled and the deflection, rotational angle and the resultant force and moment were expressed only in the terms of this new function. Simsek and Kocaturk (2009) have investigated the free and forced vibration characteristics of an FG Euler-Bernoulli beam under a moving harmonic load. Simsek (2010a) studied the free vibration analysis of an FG beam using different higher order beam theories. In a recent study, Simsek (2010b) has studied the dynamic deflections and the stresses of an FG simply-supported beam subjected to a moving mass by using Euler-Bernoulli, Timoshenko and the parabolic shear deformation beam theory. Thai *et al.* (2012) has studied the bending and free vibration of functionally graded beams using various higher-order shear deformation beam theories. Hadji *et al*. (2016) investigated the bending analysis of FGM plates using a sinusoidal shear deformation theory. Hadji (2017) used a sinusoidal shear deformation theory of functionally graded plates.

In this paper, a refined shear deformation beam theory is used to analyze the static characteristic of functionally graded beams. The present refined theory is based on assumption that the in-plane and transverse displacements consist of bending and shear components, in which the bending components do not contribute toward shear forces and, likewise, the shear components do not contribute toward bending moments. The most interesting feature of this theory is that it accounts for a parabolic variation of the transverse shear strains across the thickness and satisfies the zero traction boundary conditions on the top and bottom surfaces of the beam without using shear correction factors. The material properties of FG beam are assumed to vary according to a power law distribution of the volume fraction of the constituents. To simplify the governing equations for the FG beams, the coordinate system is located at the physical neutral surface of the beam. This is due to the fact that the stretching - bending coupling in the constitutive equations of an FG beam does not exist when the physical neutral surface is considered as a coordinate system

*Corresponding author, Ph.D.
E-mail: had_laz@yahoo.fr

ISSN: 1225-4568 (Print), 1598-6217 (Online)

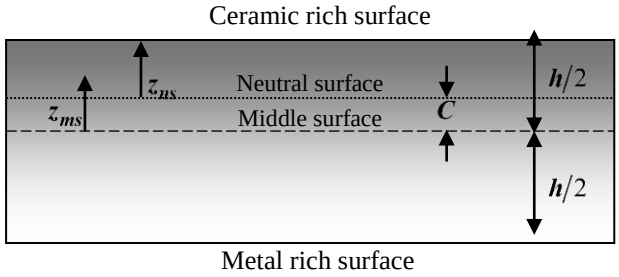

Fig. 1 The position of middle surface and neutral surface for a functionally graded beam

(Yahoobi and Feraidoon 2010, Bouremana *et al*. 2013, Klouche Djedid *et al.* 2014). Thus, the present refined beam theory based on the exact position of neutral surface together with virtual work principle is employed to extract the equilibrium equations of the FG beams. Analytical solutions are obtained for simply supported beam, and its accuracy is verified by comparing the obtained results with those reported in the literature.

2. Mathematical formulation

Consider a functionally graded beam with length L and rectangular cross section $b\times h$, with b being the width and h being the height. Since in functionally graded beams the condition of mid-plane symmetry does not exist, the stretching and bending equations are coupled. But, if the origin of the coordinate system is suitably selected in the thickness direction of the FG beam so as to be the neutral surface, the analysis of the FG beams can easily be treated with the homogenous isotropic beam theories, because the stretching and bending equations of the beam are not coupled. In order to determine the position of neutral surface of FG beams, two different datum planes are considered for the measurement of z, namely, z_{ms} and z_{ns} measured from the middle surface and the neutral surface of the beam, respectively, as shown in Fig. 1.

The volume-fraction of ceramic V_C is expressed based on z_{ms} and z_{ns} coordinates as

$$V_C = \left(\frac{z_{ms}}{h}+\frac{1}{2}\right)^k = \left(\frac{z_{ns}+C}{h}+\frac{1}{2}\right)^k \tag{1}$$

Material non-homogeneous properties of a functionally graded material beam may be obtained by means of the Voigt rule of mixture (Suresh and Mortensen 1998). Thus, using Eq. (1), the material non-homogeneous properties of FG beam P, as a function of thickness coordinate, become

$$P(z) = P_M + P_{CM}\left(\frac{z_{ns}+C}{h}+\frac{1}{2}\right)^k, \quad P_{CM} = P_C - P_M \tag{2}$$

where P_M and P_C are the corresponding properties of the metal and ceramic, respectively, and k is the material parameter which takes the value greater or equal to zero. Also, the parameter C is the distance of neutral surface from the middle surface. In the present work, we assume that the elasticity modules E is described by Eq. (2), while Poisson's ratio v, is considered to be constant across the thickness. The position of the neutral surface of the FG beam is determined to satisfy the first moment with respect to Young's modulus being zero as follows (Ould Larbi *et al*. 2013, Bouremana *et al*. 2013)

$$\int_{-h/2}^{h/2} E(z_{ms})(z_{ms}-C)dz_{ms} = 0, \tag{3}$$

Consequently, the position of neutral surface can be obtained as

$$C = \frac{\int_{-h/2}^{h/2} E(z_{ms}) z_{ms} dz_{ms}}{\int_{-h/2}^{h/2} E(z_{ms}) dz_{ms}}, \tag{4}$$

It is clear that the parameter C is zero for homogeneous isotropic beams, as expected.

2.1 Basic assumptions

The assumptions of the present theory are as follows:

- The origin of the Cartesian coordinate system is taken at the neutral surface of the FG beam.
- The displacements are small in comparison with the height of the beam and, therefore, strains involved are infinitesimal.
- The transverse displacement w includes two components of bending w_b, and shear w_s. These components are functions of coordinates x, y only.

$$w(x, z_{ns}) = w_b(x) + w_s(x) \tag{5}$$

- The transverse normal stress σ_z is negligible in comparison with in-plane stresses σ_x. The axial displacement u in x-direction, consists of extension, bending, and shear components.

$$u = u_0 + u_b + u_s \tag{6}$$

- The bending component u_b is assumed to be similar to the displacements given by the classical beam theory. Therefore, the expression for u_b can be given as

$$u_b = -z_{ns}\frac{\partial w_b}{\partial x} \tag{7}$$

- The shear component u_s gives rise, in conjunction with w_s, to the hyperbolic variation of shear strain γ_{xz} and hence to shear stress τ_{xz} through the thickness of the beam in such a way that shear stress τ_{xz} is zero at the top and bottom faces of the beam. Consequently, the expression for u_s can be given as

$$u_s = -f(z_{ns})\frac{\partial w_s}{\partial x} \tag{8}$$

where

$$f(z_{ns}) = (z_{ns}+C)\left(1-\cosh\left(\frac{1}{2}\right)\right) + h\sinh\left(\frac{z_{ns}+C}{h}\right) \tag{9}$$

2.2 Kinematics and constitutive equations

Based on the assumptions made in the preceding section, the displacement field can be obtained using Eqs. (5)-(9) as

$$u(x,z_{ns}) = u_0(x) - z_{ns}\frac{\partial w_b}{\partial x} - f(z_{ns})\frac{\partial w_s}{\partial x} \tag{10a}$$

$$w(x,z_{ns}) = w_b(x) + w_s(x) \tag{10b}$$

The strains associated with the displacements in Eq. (10) are

$$\varepsilon_x = \varepsilon_x^0 + z_{ns}\,k_x^b + f(z_{ns})\,k_x^s \tag{11a}$$

$$\gamma_{xz} = g(z_{ns})\,\gamma_{xz}^s \tag{11b}$$

where

$$\varepsilon_x^0 = \frac{\partial u_0}{\partial x},\quad \mathrm{k_x^b} = -\frac{\partial^2 \mathrm{w_b}}{\partial \mathrm{x}^2},\quad \mathrm{k_x^s} = -\frac{\partial^2 \mathrm{w_s}}{\partial \mathrm{x}^2},\quad \gamma_{\mathrm{xz}}^{\mathrm{s}} = \frac{\partial \mathrm{w_s}}{\partial \mathrm{x}} \tag{11c}$$

$$g(z_{ns}) = 1 - \frac{df(z_{ns})}{dz_{ns}} \tag{11d}$$

By assuming that the material of FG beam obeys Hooke's law, the stresses in the beam become

$$\sigma_x = Q_{11}(z_{ns})\,\varepsilon_x \quad \text{and} \quad \tau_{xz} = Q_{55}(z_{ns})\,\gamma_{xz} \tag{12a}$$

where

$$Q_{11}(z_{ns}) = E(z_{ns}) \quad \text{and} \quad Q_{55}(z_{ns}) = \frac{E(z_{ns})}{2(1+\nu)} \tag{12b}$$

2.3 Governing equations

The governing equations of equilibrium can be derived by using the principle of virtual displacements. The principle of virtual work in the present case yields

$$\int_0^L \int_{-\frac{h}{2}-C}^{\frac{h}{2}-C} \left(\sigma_x \delta\varepsilon_x + \tau_{xz}\delta\gamma_{xz}\right) dz_{ns}\,dx - \int_0^l q\left(\delta w_b + \delta w_s\right) dx = 0 \tag{13}$$

Substituting Eqs. (11) and (12) into Eq. (13) and integrating through the thickness of the beam, Eq. (13) can be rewritten as

$$\int_0^L \left(N\frac{d\delta u_0}{dx} - M_b\frac{d^2\delta w_b}{dx^2} - M_s\frac{d^2\delta w_s}{dx^2} + Q\frac{d\delta w_s}{dx}\right) dx - \int_0^l q\left(\delta w_b + \delta w_s\right) dx = 0 \tag{14}$$

where N, M_b, M_s and Q are the stress resultants defined as

$$(N, M_b, M_s) = \int_{-\frac{h}{2}-C}^{\frac{h}{2}-C} (1, z_{ns}, f)\,\sigma_x\,dz_{ns} \quad \text{and} \qquad Q = \int_{-\frac{h}{2}-C}^{\frac{h}{2}-C} g\,\tau_{xz}\,dz_{ns} \tag{15}$$

The governing equations of equilibrium can be derived from Eq. (14) by integrating the displacement gradients by parts and collecting the coefficients of δu_0, δw_b and δw_s, the following equations of equilibrium of the functionally graded beam are obtained

$$\begin{aligned} \delta u_0 &: \ \frac{dN}{dx} = 0 \\ \delta w_b &: \ \frac{d^2 M_b}{dx^2} + q = 0 \\ \delta w_s &: \ \frac{d^2 M_s}{dx^2} + \frac{dQ}{dx} + q = 0 \end{aligned} \tag{16}$$

Eq. (16) can be expressed in terms of displacements (u_0, w_b, w_s) by using Eqs. (10), (11), (12) and (15) as follows

$$A_{11}\frac{\partial^2 u_0}{\partial x^2} - B_{11}^s\frac{\partial^3 w_s}{\partial x^3} = 0 \tag{17a}$$

$$-D_{11}\frac{\partial^4 w_b}{\partial x^4} - D_{11}^s\frac{\partial^4 w_s}{\partial x^4} + q = 0 \tag{17b}$$

$$B_{11}^s\frac{\partial^3 u_0}{\partial x^3} - D_{11}^s\frac{\partial^4 w_b}{\partial x^4} - H_{11}^s\frac{\partial^4 w_s}{\partial x^4} + A_{55}^s\frac{\partial^2 w_s}{\partial x^2} + q = 0 \tag{17c}$$

where A_{11}, D_{11}, etc., are the beam stiffness, defined by

$$\left(A_{11}, D_{11}, B_{11}^s, D_{11}^s, H_{11}^s\right) = \int_{-\frac{h}{2}-C}^{\frac{h}{2}-C} Q_{11}\left(1, z^2, f(z_{ns}), z_{ns}\,f(z_{ns}), f^2(z_{ns})\right) dz_{ns} \tag{18a}$$

and

$$A_{55}^s = \int_{-\frac{h}{2}-C}^{\frac{h}{2}-C} Q_{55}\left[g(z_{ns})\right]^2 dz_{ns}, \tag{18b}$$

3. Analytical solution

The equilibrium equations admit the Navier solutions for simply supported beams. The variables u_0, w_b, w_s can be written by assuming the following variations

$$\begin{Bmatrix} u_0 \\ w_b \\ w_s \end{Bmatrix} = \sum_{m=1}^{\infty} \begin{Bmatrix} U_m \cos(\lambda x) \\ W_{bm}\sin(\lambda x) \\ W_{sm}\sin(\lambda x) \end{Bmatrix} \tag{19}$$

where U_m, W_{bm}, and W_{sm} are arbitrary parameters to be determined, and $\lambda=m\pi/L$. The transverse load q is also expanded in Fourier series as

$$q(x)=\sum_{m=1}^{\infty}Q_m \sin(\lambda x) \tag{20}$$

where Q_m is the load amplitude calculated from

$$Q_m=\frac{2}{L}\int_0^L q(x)\sin(\lambda x)dx \tag{21}$$

The coefficients Q_m are given below for some typical loads. For the case of a sinusoidally distributed load, we have

$$m=1 \text{ and } Q_1=q_0 \tag{22a}$$

and for the case of uniform distributed load, we have

$$Q_m=\frac{4q_0}{m\pi},\ (m=1,3,5....) \tag{22b}$$

Substituting the expansions of u_0, w_b, w_s and q from Eqs. (19) and (20) into the equations of motion Eq. (17), the analytical solutions can be obtained from the following equations

$$\begin{bmatrix} a_{11} & 0 & a_{13} \\ 0 & a_{22} & a_{23} \\ a_{13} & a_{23} & a_{33} \end{bmatrix}\begin{Bmatrix} U_m \\ W_{bm} \\ W_{sm} \end{Bmatrix}=\begin{Bmatrix} 0 \\ Q_m \\ Q_m \end{Bmatrix} \tag{23}$$

where

$$\begin{gathered} a_{11}=A_{11}\lambda^2,\ a_{13}=-B_{11}^s\lambda^3,\ a_{22}=D_{11}\lambda^4, \\ a_{23}=D_{11}^s\lambda^4,\ a_{33}=H_{11}^s\lambda^4+A_{55}^s\lambda^2 \end{gathered} \tag{24}$$

4. Numerical results

In this section, various numerical examples are presented and discussed to verify the accuracy of the present theory in predicting the bending responses of simply supported FG beams. The FG beam is taken to be made of aluminum and alumina with the following material properties:

Ceramic (P_C: Alumina, Al_2O_3): E_c=380 GPa; v=0.3.

Metal (P_M: Aluminium, Al): E_m=70 GPa; v=0.3.

For convenience the following forms are used:

$$\bar{w}=100\frac{E_m h^3}{q_0 L^4}w\left(\frac{L}{2}\right),\quad \bar{u}=100\frac{E_m h^3}{q_0 L^4}u\left(0,-\frac{h}{2}-C\right),$$

$$\bar{\sigma}_x=\frac{h}{q_0 L}\sigma_x\left(\frac{L}{2},\frac{h}{2}-C\right),\quad \bar{\tau}_{xz}=\frac{h}{q_0 L}\tau_{xz}(0,-C),$$

4.1 Comparison of displacement, normal stresses and shear stresses

Example 1:

Table 1 contain non-dimensional Deflection, Normal Stresses and Shear Stresses of functionally graded beam under uniform load q for power-law index k and span to depth ratio L/h. the obtained results are compare with other shear deformation theories. (Ould Larbi and Hadji).

Table 1 Nondimensional displacements and stresses of FG beams under uniform load

k	Method	L/h=5				L/h=20			
		$\bar{u}$	$\bar{w}$	$\bar{\sigma}_x$	$\bar{\tau}_{xz}$	$\bar{u}$	$\bar{w}$	$\bar{\sigma}_x$	$\bar{\tau}_{xz}$
0	Present	0.9397	3.1655	3.8016	0.7310	0.2305	2.8962	15.0128	0.7415
	Ould Larbi *et al.* (2013)	0.9406	3.1651	3.8043	0.7489	0.2305	2.8962	15.0136	0.7625
	Hadji *et al.* (2014)	0.9400	3.1654	3.8019	0.7330	0.2305	2.8962	15.0129	0.7437
1	Present	2.3036	6.2593	5.8829	0.7310	0.5685	5.8049	23.2050	0.7415
	Ould Larbi *et al.* (2013)	2.3052	6.2590	5.8875	0.7489	0.5685	5.8049	23.2063	0.7625
	Hadji *et al.* (2014)	2.3038	6.2594	5.8835	0.7330	0.5685	5.8049	23.2051	0.7437
2	Present	3.1129	8.0686	6.8817	0.6683	0.7691	7.4421	27.0987	0.67893
	Ould Larbi *et al.* (2013)	3.1146	8.0683	6.8878	0.6870	0.7691	7.4421	27.1005	0.7005
	Hadji *et al.* (2014)	3.1129	8.0677	6.8824	0.6704	0.7691	7.4421	27.0989	0.6812
5	Present	3.7097	9.8273	8.1092	0.5881	0.9134	8.8182	31.8124	0.5988
	Ould Larbi *et al.* (2013)	3.7128	9.8345	8.1187	0.6084	0.9134	8.8186	31.8151	0.6218
	Hadji *et al.* (2014)	3.7100	9.8281	8.1104	0.5904	0.9134	8.8182	31.8127	0.6013
10	Present	3.8859	10.9374	9.7109	0.6443	0.9536	9.6906	38.1379	0.6561
	Ould Larbi *et al.* (2013)	3.8898	10.9413	9.7203	0.6640	0.9537	9.6907	38.1408	0.6788
	Hadji *et al.* (2014)	3.8863	10.9381	9.7119	0.6465	0.9536	9.6905	38.1382	0.6586

Example 2:

Table 2 and Table 3 contains non-dimensional Deflection, Normal Stresses and Shear Stresses of functionally graded beam under Sinusoidal Load q_0 for power-law index k and span to depth ratio L/h.

4.2 Discussion

4.2.1 Inplane displacement ū

The variation of inplane displacement ū through the thickness of beam is given in Fig. 2, Fig. 3, Fig. 4 and Fig. 5 for uniform and sinusoidal load for aspect ratio 5 and 20 for different fraction exponent k. The through thickness variation given by the present theory for Ceramic is observed to be linear. The inplane displacements obtained by the present theory are compared with those of Ould larbi

Table 2 Nondimensional displacements and stresses of FG beams under sinusoidal load (*L*/*h*=5)

k	Method	*L*/*h*=5			
		$\bar{u}$	$\bar{w}$	$\bar{\sigma}_x$	$\bar{\tau}_{xz}$
0	Present	0.7250	2.5020	3.0913	0.4755
	Reddy*	0.7251	2.5020	3.0916	0.4769
	Timoshenko**	0.7129	2.5023	3.0396	0.3183
	CBT"	0.7129	2.2693	3.0396	-
1	Present	1.7792	4.9458	4.7851	0.4755
	Reddy*	1.7793	4.9458	4.7856	0.5243
	Timoshenko**	1.7588	4.8807	4.6979	0.5376
	CBT"	1.7588	4.5528	4.6979	-
5	Present	2.8641	7.7715	6.6047	0.3840
	Reddy*	2.8644	7.7723	6.6057	0.5314
	Timoshenko**	2.8250	7.5056	6.4382	0.9942
	CBT"	2.8250	6.8994	6.4382	-
10	Present	2.9986	8.6526	7.9069	0.4208
	Reddy*	2.9989	8.6530	7.9080	0.4236
	Timoshenko**	2.9488	8.3259	7.7189	1.2320
	CBT"	2.9488	7.5754	7.7189	-

*Results form Ref (Reddy 1984)
**Results form Ref (Timoshenko 1921)
"Results form Ref (Euler 1744)

Table 3 Nondimensional displacements and stresses of FG beams under sinusoidal load (*L*/*h*=20)

k	Method	*L*/*h*=20			
		$\bar{u}$	$\bar{w}$	$\bar{\sigma}_x$	$\bar{\tau}_{xz}$
0	Present	0.1784	2.2839	12.1715	0.4760
1	Present	0.4400	4.5774	18.8136	0.4760
5	Present	0.7068	6.9539	25.7944	0.3847
10	Present	0.7380	7.6421	30.9227	0.4215

et al. (2013), Hadji *et al*. (2014). The value obtained by present theory is in excellent agreement with other theories.

4.2.2 Transverse displacement $\bar{w}$

The variation of central transverse displacement $\bar{w}$ for aspect ratios 5 and 20 is presented in Table 1 and Table 2 for beams subjected to uniform load and for beams subjected to sinusoidal load in Table 3 and Table 4 for various aspect ratios *L*/*h*. The value of transverse displacement obtained by the present theory is in excellent agreement with results of Hadji *et al.* (2014) and theorie of Ould Larbi *et al*. (2013). The deflections predicted by the CPT are less than those given by present shear deformation theory; due to the neglect effect of shear deformation.

4.2.3 Inplane normal stress $\bar{\sigma}_x$

The maximum inplane normal stress obtained by the present theory is compared with those of Hadji and the refined theorie of Ould Larbi.

The maximum value obtained by present theory is in excellent agreement with other theories. As per the Table 1, Table 2, Table 3 and Table 4 as the aspect ratio increases,

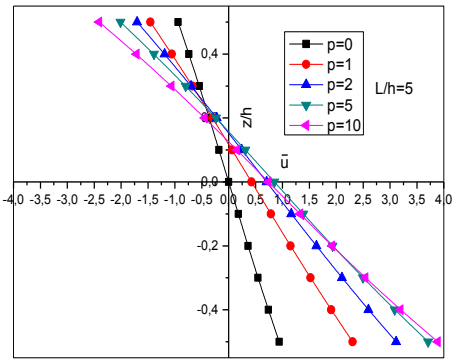

Fig. 2 Through thickness variation of $\bar{u}$ for functionally graded beam subjected to UDL for aspect ratio (*L*/*h*=5)

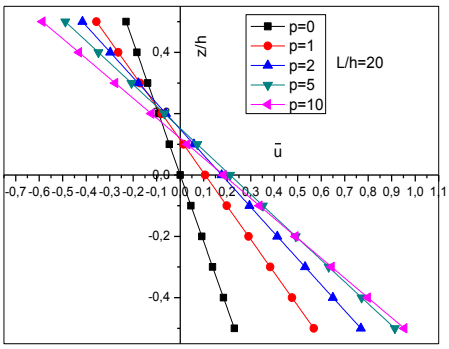

Fig. 3 Through thickness variation of $\bar{u}$ for functionally graded beam subjected to UDL for aspect ratio (*L*/*h*=20)

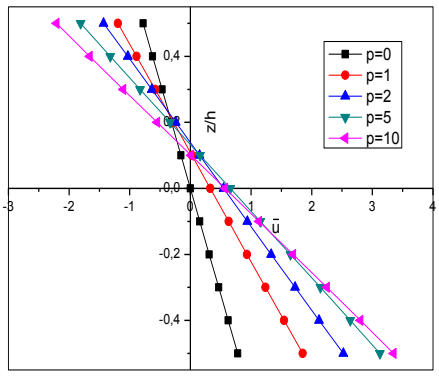

Fig. 4 Through thickness variation of $\bar{u}$ for functionally graded beam subjected to SSL for aspect ratio (*L*/*h*=5)

the inplane normal stress also increases for uniform load and sinusoidal load for FG beam.

The present theory gives linear variation of this stress through the thickness as shown in Fig.6 for Ceramic and Curved for other fraction exponent identical to other refined theories.

4.2.4 Transverse shear stress $\bar{\tau}_{xz}$

For the FG beam the transverse shear stresses are in excellent agreement with those obtained by other refined theories. The present theory shows exact variation of this stress through the thickness as shown in Fig. 10, Fig. 11, Fig. 12 and Fig. 13 for ceramic and other fraction exponent

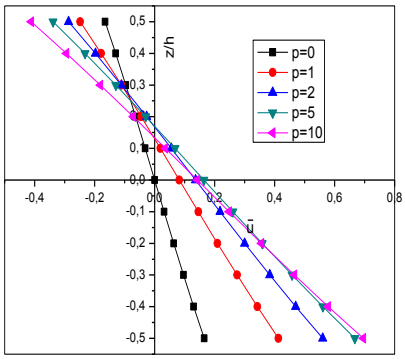

Fig. 5 Through thickness variation of $\bar{u}$ for functionally graded beam subjected to SSL for aspect ratio (L/h=20)

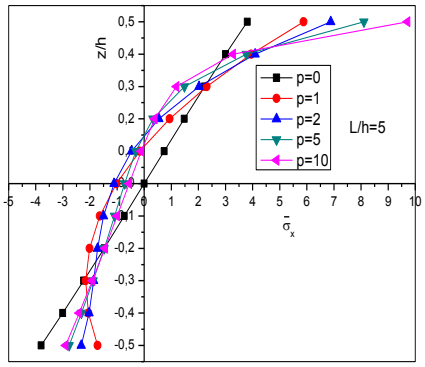

Fig. 6 Through thickness variation of $\bar{\sigma}_x$ for functionally graded beam subjected to UDL for aspect ratio (L/h=5)

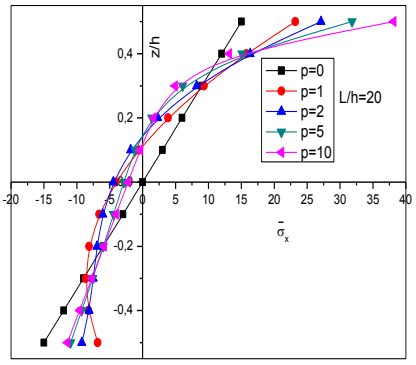

Fig. 7 Through thickness variation of $\bar{\sigma}_x$ for functionally graded beam subjected to UDL for aspect ratio (L/h=20)

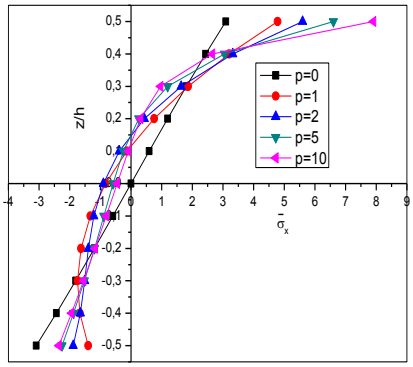

Fig. 8 Through thickness variation of $\bar{\sigma}_x$ for functionally graded beam subjected to SSL for aspect ratio (L/h=5)

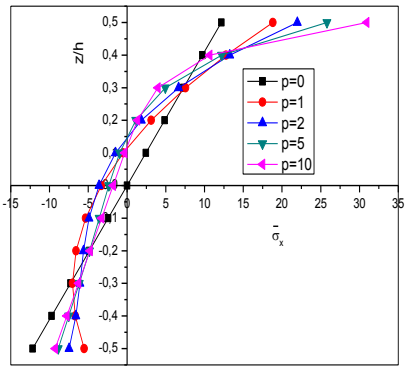

Fig. 9 Through thickness variation of $\bar{\sigma}_x$ for functionally graded beam subjected to SSL for aspect ratio (L/h=20)

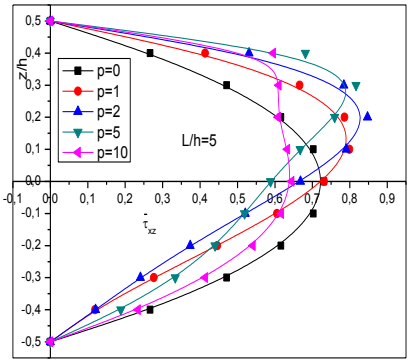

Fig. 10 Through thickness variation of $\bar{\tau}_{xz}$ for functionally graded beam subjected to UDL for aspect ratio (L/h=5)

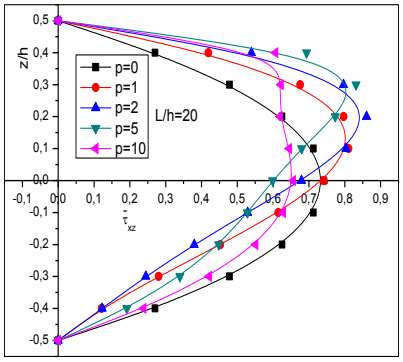

Fig. 11 Through thickness variation of $\bar{\tau}_{xz}$ for functionally graded beam subjected to UDL for aspect ratio (L/h=20)

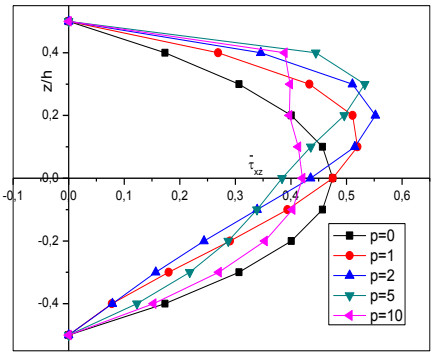

Fig. 12 Through thickness variation of $\bar{\tau}_{xz}$ for functionally graded beam subjected to SSL for aspect ratio (L/h=5)

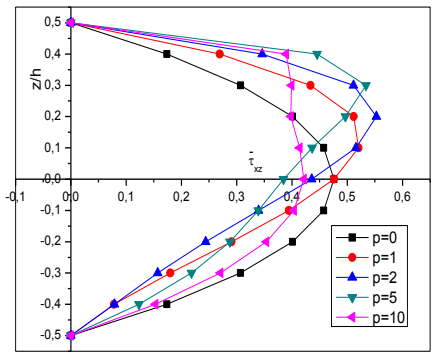

Fig. 13 Through thickness variation of $\bar{\tau}_{xz}$ for functionally graded beam subjected to SSL for aspect ratio (L/h=20)

identical to other refined theories which gives the parabolic curve under uniform and sinusoidal load.

5. Conclusions

A refined hyperbolic shear deformation beam theory is proposed to analyze the bending of functionally graded beams. The present theory is variationally consistent, uses the hyperbolic term to represent the displacement field, does not require shear correction factor, and gives rise to transverse shear stress variation such that the transverse shear stresses vary parabolically across the thickness satisfying shear stress free surface conditions. It is based on the assumption that the transverse displacements consist of bending and shear components in which the bending components do not contribute toward shear forces and, likewise, the shear components do not contribute toward bending moments. Based on the present beam theory and the neutral surface concept, the equilibrium equations are derived from the principle of virtual work. Numerical examples show that the proposed theory gives solutions which are almost identical with those obtained using other shear deformation theories.

References

Bouremana, M., Houari, M.S.A., Tounsi, A., Kaci, A., Adda Bedia, E.A. (2013), "A new first shear deformation beam theory based on neutral surface position for functionally graded beams", *Steel and Composite Structures*, **15**(5), 467- 479.

Euler, L. (1744), *Methodus Inveniendi Lineas Curvas Maximi Minimive Proprietate Gaudentes*, Lausanne and Geneva.

Hadji, L., Daouadji, T.H., Tounsi, A. and Adda bedia, E.A. (2014), "A higher order shear deformation theory for static and free vibration of FGM beam", *Steel Compos. Struct.*, **16**(5), 507-519.

Hadji, L., Zouatnia, N. and Kassoul, A. (2016), "Bending analysis of FGM plates using a sinusoidal shear deformation theory", *Wind Struct.*, **23**(6), 543-558.

Hadji, L. (2017), "Analysis of functionally graded plates using a sinusoidal shear deformation theory", *Smart Struct. Syst.*, **19**(4), 441-448.

Klouche Djedid, I., Benachour, A., Houari, M.S.A., Tounsi, A. and Ameur, M. (2014), "A n-order four variable refined theory for bending and free vibration of functionally graded plates", *Steel Compos. Struct.*, **17**(1), 21-46.

Li, X.F. (2008), "A unified approach for analyzing static and dynamic behaviors of functionally graded Timoshenko and Euler-Bernoulli beams", *J. Sound Vib.*, **318**, 1210-1229.

Ould Larbi, L., Kaci, A., Houari, M.S.A. and Tounsi, A. (2013), "An efficient shear deformation beam theory based on neutral surface position for bending and free vibration of functionally graded beams", *Mech. Bas. Des. Struct. Mach.*, **41**, 421-433.

Reddy, J.N. (1984), "A Simple higher order theory for laminated composites plates", *ASME J. Appl. Mech.*, **51**, 745-752.

Simsek, M. and Kocaturk, T. (2009), "Free and forced vibration of a functionally graded beam subjected to a concentrated moving harmonic load", *Compos. Struct.*, **90**(4), 465-473.

Simsek, M. (2010a), "Fundamental frequency analysis of functionally graded beams by using different higher-order beam theories", *Nucl. Eng. Des.*, **240**(4), 697-705.

Simsek, M. (2010b), "Vibration analysis of a functionally graded beam under a moving mass by using different beam theories", *Compos. Struct.*, **92**(4), 904-917.

Thai, H.T. and Vo, T.P. (2012), "Bending and free vibration of functionally graded beams using various higher-order shear deformation beam theories", *Int. J. Mech. Sci.*, **62**, 57-66.

Timoshenko, S.P. (1921), "On the correction for shear of the differential equation for transverse vibration of prismatic bars", *Phil. Mag. Ser. 6*, **46**, 744-746.

Yaghoobi, H. and Yaghoobi, P. (2013), "Buckling analysis of sandwich plates with FGM face sheets resting on elastic foundation with various boundary conditions: An analytical approach", *Meccanica*, **48**, 2019-2039.

PL